www.czasopisma.pan.pl PAN www.journals.pan.pl

ARCHIVES of FOUNDRY ENGINEERING

ISSN (2299-2944)
Volume 2023
Issue 3/2023

30 – 37

10.24425/afe.2023.144312

5/3

Published quarterly as the organ of the Foundry Commission of the Polish Academy of Sciences

Effectiveness of Absorbing Microwaves by the Multimaterial Sodium Silicate Base Sand - PLA (Polylactide) Mould Wall Systems

M. Stachowicz
Wroclaw University of Technology, Poland
Corresponding author: mateusz.stachowicz@pwr.edu.pl

Received 17.04.2023; accepted in revised form 27.05.2023; available online 31.07.2023

Abstract

In the paper presented are results of a research on effectiveness of absorbing electromagnetic waves at frequency 2.45 GHz by unhardened sodium silicate base sands (SSBS) prepared of high-silica base sand and a PLA (Polylactide) 3D-prited (3DP) mould walls. Measurements of power loss of microwave radiation (P_{in}) expressed by a total of absorbed power (P_{abs}), output power (P_{out}) and reflected power (P_{ref}) were carried-out on a stand of semiautomatic microwave slot line for determining balance of microwave power emitted into selected multimaterial systems. Values of microwave power loss in the rectangular waveguide filled with unhardened moulding sands and prepared by fused deposition modelling (FDM) 5 mm polylactide (PLA) walls with grid infill density from 25% to c.a. 100% served for determining effectiveness of microwave heating. Balance of microwave power loss is of technological importance for microwave manufacture of high-quality casting sand moulds and cores in possibility of use 3D-printed mould tools and core boxes. It was found that apparent density of SSBS placed in a waveguide with PLA walls influences parameters of power output (P_{out}) and power reflected (P_{ref}). The PLA wall position and grid infill density were identified to have a limited effect on effectiveness of absorbing microwaves (P_{abs}).

Key words: Foundry, Microwaves, Sodium silicate base sand, PLA, Lossiness measurements

1. Introduction

In previous research works on absorption of 2.45 GHz microwaves [1-3] the semiautomatic test stand used in the research, i.e. working in Wroclaw University of Technology the microwave slot line, can be successfully used for precise examinations of microwave (MW) power loss in the waveguide filled with moulding sands prepared with inorganic binder (SSBS). For this purpose, helpful are measurements of MW radiation lossiness factors (Fig. 1) like RL and IL [4], which are defined as:

– return loss (RL) factor defines the MW field energy lost by primary reflections from the substrate surfaces present on propagation way of MW standing wave in transmission slot line;
– insertion loss (IL) factor defines the MW field energy dissipated in the transmission slot line.

Determination of these two factors (IL, RL) make possible to calculate shares of: absorbed MW power (P_{abs}), reflected power (P_{ref}) and output power (P_{out}) during transition through the examined multimaterial system. In the case of using MW for hardening (curing) [5-7] of eco-friendly, inorganic sodium silicate (so-called water-glass) [8-10] moulding and core sands, basic parameters informing about effectiveness of the process should be determined. These parameters are: value of losses related to incidence and reflection of microwaves from the surface (walls) on their

propagation way, value of losses related to dissipation of microwaves inside the waveguide and transmission losses related to instrumentation materials, in particular waveguides and microwave chambers (Fig. 1).

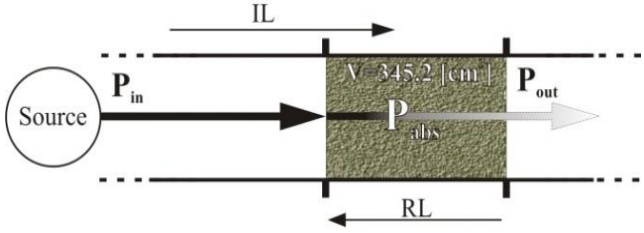

Fig. 1. Propagation of electromagnetic wave in a rectangular waveguide

Effectiveness of heating of unhardened moulding sands and other materials, like used in the foundry tooling [1]: pine wood, textolite, polytetrafluoroethylene (PTFE) and recycled polytetrafluoroethylene (rPTFE) were positively examined in multimaterial "moulding sand – foundry instrumentation" systems. Mentioned materials are preferred for tools working in MW field, but purchasing, machining, manufacturing and assembling are cost and time high. To low manufacturing costs in one-off and a small batch production the role of 3D-pritned elements is playing an increasingly important role.

Due to availability and low equipment and material costs one of the most widely used additive manufacturing (AM) techniques is fused deposition modelling (FDM). FDM technology allows for the use of a wide spectrum of thermoplastic materials, i.e. polyethylene terephthalate modified with glycol (PETG), thermoplastic polyurethane (TPU), acrylonitrile-butadiene-styrene (ABS), nylon (PA), and biodegradable polyester such as polylactide (polylactic acid) known as PLA. Polylactide is a semi crystalline thermoplastic and it's is one of the easiest materials to print i.e. for prototypes, small and large models, core boxes where high mechanical, chemical, or temperature resistance aren't require. Also PLA-made elements gets soft and may deform at temperatures over 60 °C. PLA thermal degradation can be occurred in the temperature range of 300 – 500°C [11]. Mechanical parameters of 3D-printed (3DP) parts depends on variable FDM process parameters, such as: printing speed and extruder and table temperatures, infill density and pattern type [12], layer height and layer width. All of mentioned parameters can be modified to generate the optimal values for their users. Due to the small loss tangent (tanδ) [13], low costs [11] and low adhesion to other materials PLA was chosen to be examined at first in microwave field (2.45 GHz) as a multimaterial: sodium silicate base sand - PLA (Polylactide) mould box wall system.

The research presented in this paper are aimed on determination of effectiveness of absorbing microwaves by the multimaterial sodium silicate base sand - PLA (Polylactide) mould wall systems carried-out using a stand of semiautomatic microwave slot line for measurements of the standing wave ratio (SWR). The research results should help in the selection of suitable materials for casting tooling, which include moulding and core boxes.

2. Materials and Methods

2.1. Semiautomatic microwave slot line

Lossiness factors such as: insertion loss (IL) and return loss (RL) are determine by measuring maximum amplitude of the sinusoidal standing wave [4] generated in a rectangular aluminium waveguide filled with a unhardened sodium silicate boned sand (SSBS) and other materials, like a PLA walls. For very precise determination of standing wave ratio (SWR) value for calculations of RL and IL factors the MW power was established on the level of ca. 3.98 mW. Low level of MW power reduced to a minimum the possibility of heating the examined SSBS. Generated in slot line stand MW amplitude values were recorded in a function of voltage (mV) by the diode detector with sensitivity level not below 0.4 mV. The lossiness factors (IL and RL) caused by the multimaterial systems present in the measuring chamber waveguide are determined by two equations (1) and (2), which are showed below:

$$RL = 20\log\left|s_{11}\right| \ [\text{dB}] \tag{1}$$

$$IL = 10\log\left|s_{21}\right| \ [\text{dB}] \tag{2}$$

Measured in the slot line lossiness factors gives the possibility to calculate microwave absorption share (P_{abs}) with use of the equation (3):

$$P_{abs} = \left(1 - (10^{\left(\frac{IL}{10}\right)} + 10^{\left(\frac{RL}{10}\right)})\right) \cdot 100\ [\%] \tag{3}$$

Power balance (P_{in}) of MW acting on the multimaterial SSBS-PLA system is presented in the equation (4), which is useful to validity [14] of the equation (3). In general, MW power (P_{in}) of microwaves propagating in the slot line waveguide filled with the examined multimaterial system is the sum of three components:

$$P_{in} = P_{abs} + P_{ref} + P_{out} \tag{4}$$

where P_{ref} means reflected power and P_{out} means output power after transition through the examined multimaterial SSBS-PLA system located in the measuring chamber (Fig. 1). Share of P_{ref} is expressed by the equation (5) and the share of output power (P_{out}) by the equation (6):

$$P_{ref} = \left(10^{\left(\frac{RL}{10}\right)}\right) \cdot 100\ [\%] \tag{5}$$

$$P_{out} = \left(10^{\left(\frac{IL}{10}\right)}\right) \cdot 100\ [\%] \tag{6}$$

2.2. Materials

To determine the effectiveness of MW absorption of multimaterial SSBS - PLA systems, commercially available high-silica sand (Table 1) obtained from the polish mine Grudzeń Las Sp. z o.o. was used. To prepare SSBS non-modified sodium silicate

inorganic binder grade 137 from Chemical Plant Rudniki S.A. with the properties given in Table 1 was used.

A portion of 6-kg of SSBS for the examinations were prepared in a laboratory ribbon mixer in the following proportions (by mass, per 100 parts of SSBS): 0.5 part of water were dosed to the sand matrix, then 1.5 parts of binder 137 were dosed in 60 s after starting mixing. Total mixing time was 240 s. Prepared SSBS was stored under ambient conditions at temperature of 23 ±2 °C.

Compaction process of the multimaterial systems were made on the Multiserw Morek's apparatus LUZ-2e with vibration frequency at 50 Hz. Densification applied amplitudes (A) amounting to: 80%, 60% or 40% of the maximum value 2 mm of vibrations. In the tests, constant process time of 60 s and constant volume of measuring chamber of 345.2 cm^3 were proceed.

Used for 3D-printing filament is a commercially available PLA manufactured by Devil Design with given in Table 1 physical properties.

Table 1.
Parameters of examined materials in multimaterial moulding sand - PLA systems

High-silica sand acc. to PN-85/H-11001:	**Fraction 1:**	**Fraction 2:**	**Fraction 3:**
Fine	0.10	0.16	0.20
Fe / wt% max.		0.1	
Binder (sodium silicate) grade 137:			
Molar module SiO_2/Na_2O	**Oxide content (SiO_2+Na_2O) % min.**	**Density (20°C) g/cm^3**	**Fe_2O_3 % max.**	**Dynamic viscosity (P) min.**
3.4	36.3	1.37	0.02	1
PLA filament for 3DP:			
Diameter of filament:	1.75 mm +/- 0.05 mm	**Density:**	1.24 g/cm^3
Shrinkage of the material:	Very low	**Elongation at Break:**	160%
Hotend:	200-235°C	**Spencer Impact:**	2.5 joules
Heated bed:	50-60°C	**Softening temperature:**	~50°C

3DP walls with dimensions of 86 x 43 x 5 mm were designed in Autodesk Inventor Professional 2022 and exported to a .stl file format. Slicing of the 3DP walls was made in Ultimaker Cura 4.11.0 program (Fig. 2). Basic parameters of printing from ø 1.75 mm PLA filament are given in Table 2.

Table 2.
Ultimaker Cura slicer printing properties of the PLA-made moulding/core box walls

Hotend printing temperature:	218°C	**Wall thickness:**	1.0 mm
Heat bed temperature:	50°C	**Top/bottom thickness:**	1.0 mm
Layer height:	0.2 mm	**Grid infill density; G:**	25%/ 50%/ 75%/ 100%
Initial layer height:	0.2 mm	**Print speed:**	50.0 mm/s

The 5 mm thick walls were 3D-printed on Hayabusa steel frame Anet A6 printer with extruder nozzle diameter of 0.4 mm. The Hitachi TM-3000 scanning microscope was used to show the cross-section of samples with the grid-type trails (Fig. 3). The obtained surfaces of the PLA walls were examined by the method of 3D digital reconstruction of the surface after scanning microscope (SEM) imaging.

It should be noted that a chosen parameter of grid-pattern infill density at 100% in Cura slicer does not mean that after slicing the inner part of the wall will be 100% filled with PLA (Fig. 3d). The infill density has a significant role of strength of the FDM part [15, 16].

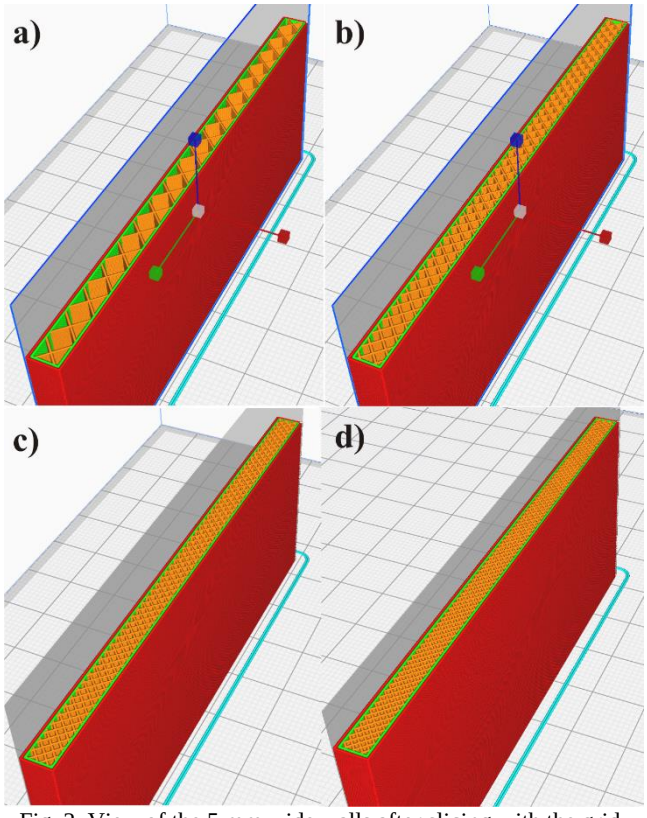

Fig. 2. View of the 5 mm wide walls after slicing with the grid-type pattern and infill density: a) 25%, b) 50%, c) 75%, d) 100%

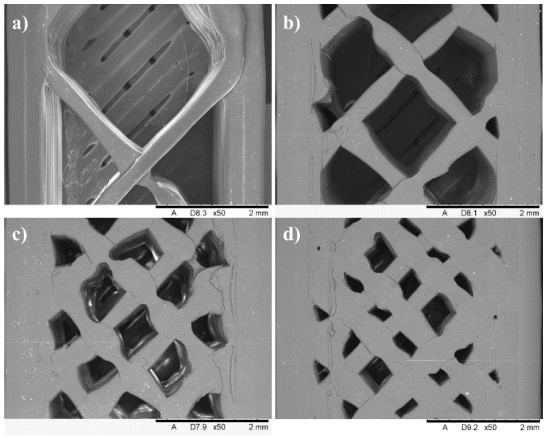

Fig. 3. View of the grid pattern trials in printed from PLA walls. Infill density: a) 25%, b) 50%, c) 75%, d) 100%. SEM microscopy

2.3. Design of Experiments

Research on effectiveness of absorbing microwaves (MW) at frequency 2.45 GHz by unhardened SSBS prepared of high-silica base sand with a 3D-printed PLA walls were spread on three V-variants:

- 1st variant (V1) where the 5 mm deep PLA wall was placed at the front of microwave source (Fig. 4), where were tested four types of infill density: V1 G:25%, V1 G:50%, V1 G:75% and G:V1 100%;
- 2nd variant (V2) where the 5 mm deep PLA walls were placed at the front and rear of the waveguide with the SSBS specimen (Fig. 5), where were tested four types of infill density: V2 G:25%, V2 G:50%, V2 G:75% and G:V2 100%;
- 3rd variant (V3) where the 5 mm deep PLA wall was placed at the end of the waveguide with the SSBS specimen (Fig. 6), where were tested four types of infill density: V3 G:25%, V3 G:50%, V3 G:75% and G:V3 100%.

Three compaction amplitudes were applied to each of these variants: A40%, A60%, A80%. Four sets of PLA walls were made on the 3D printer, two in each set.

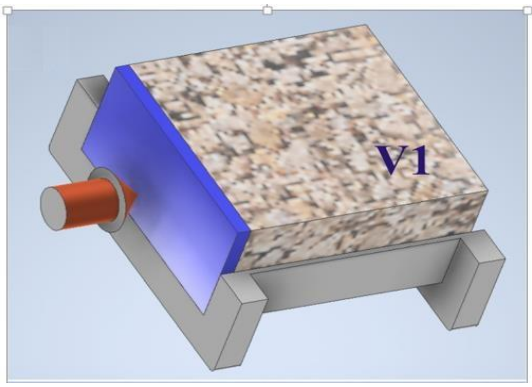

Fig. 4. Example of arrangement of 3DP PLA (marked in blue) moulding/core box wall inside a waveguide filled with moulding sand in 1st variant (V1)

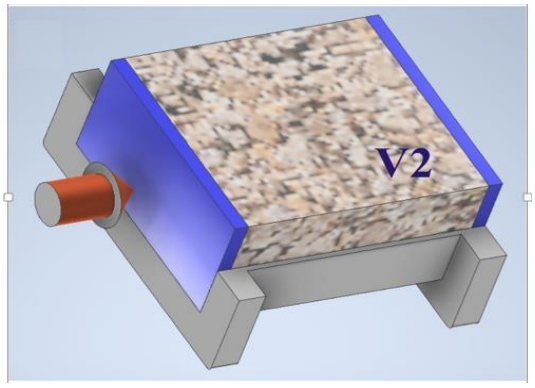

Fig. 5. Example of arrangement of 3DP PLA (marked in blue) moulding/core box walls inside a waveguide filled with moulding sand in 2nd variant (V2)

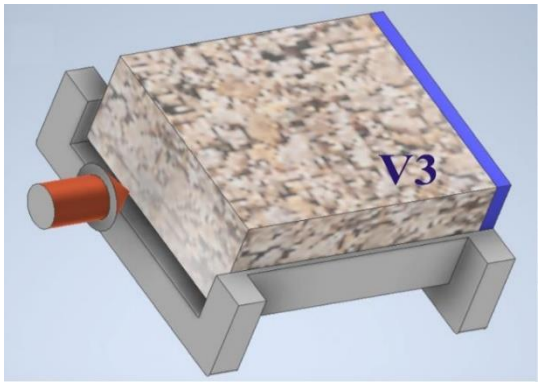

Fig 6. Example of arrangement of 3DP PLA (marked in blue) moulding/core box wall inside a waveguide filled with moulding sand in 3rd variant (V3)

3. Results

Measurement results for loss factors, which were RL and IL (given in attenuation units dB) during microwave penetration of the multimaterial SSBS - PLA system, determined in the microwave slot line chamber (Fig. 1), were converted according to the formulas (3), (5) and (6) to components of output power P_{in} (%) represented by the formula (4).

For the unhardened SSBS and 3D-printed PLA walls with four infill values, after vibratory method of compacting, power balance of microwaves (P_{in}) are shown in the Figure 7 (A40% amplitude), Figure 8 (A60% amplitude) and Figure 9 (A80% amplitude).

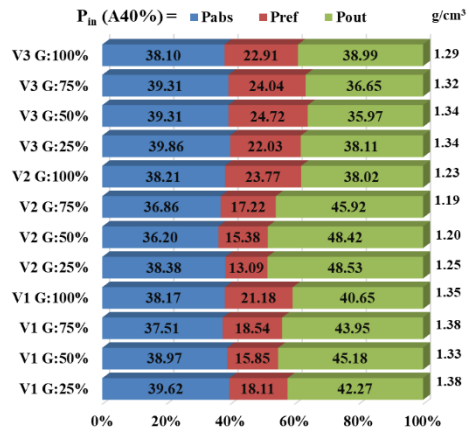

Fig. 7. P_{in} balance of microwave heating of an unhardened SSBS after A40% compacting depending on: variant of placed 3DP PLA wall/walls, grid infill density and SSBS apparent density

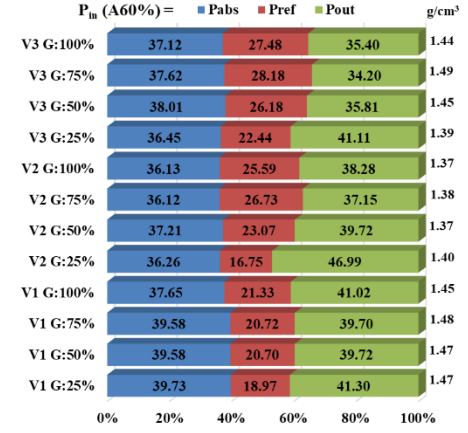

Fig. 8. P_{in} balance of microwave heating of an unhardened SSBS after A60% compacting depending on: variant of placed 3DP PLA wall/walls, grid infill density and SSBS apparent density

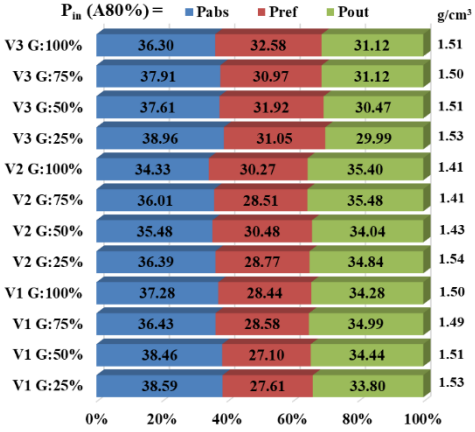

Fig. 9. P_{in} balance of microwave heating of an unhardened SSBS after A80% compacting depending on: variant of placed 3DP PLA wall/walls, grid infill density and SSBS apparent density

On the basis of the carried out studies (Figs. 7, 8, 9) of the decomposition of P_{in} into components: P_{abs}, P_{ref} and P_{out}, it can be notice that the applied compaction amplitudes A40%, A60% and A80% have an effect on the share of reflected power (P_{ref}). Changing the compaction amplitude from A40% to A80% (effect: increasing apparent density) increased the share of P_{ref} in each of analysed variant: V1, V2 and V3. The highest share of reflected power (P_{ref}) of about 30% was recorded (Fig. 9) for the systems of SSBS-PLA, where the moulding sand reached a density of 1.41 to 1.53 g/cm^3 after A80% densification. Figures 7-9 also show that changes seen in P_{ref} were also accompanied by changes in the share of power output (P_{out}), which decreased with increasing vibration amplitude at densification process. The highest contribution of P_{out} to the total P_{in} power was recorded in SSBS-PLA studies where A40% amplitudes were used. When A40% amplitudes were used, the density of SSBSs reached the value between 1.19 and 1.38 g/cm^3. The results of the microwave multimaterial systems tests confirm previous observations [4], in which an increase in the apparent SSBS density creates a trend of changes in the shares of these two (P_{ref} and P_{out}) components in the P_{in} supplied to the substrate. However, based on the described changes in the shares of P_{ref} and P_{out}, it is difficult to determine the role of the use of PLA walls in the introduced variants of: V1, V2 and V3 with different densities of grid-type filling.

Of the greatest importance for effectiveness of microwave heating is participation of power absorbed by multimaterial SSBS - PLA system, describing the part of energy to be converted to heat (P_{abs}). In order to reveal what effect the use of different V1:V3 variants and the applied grid filling inside the PLA walls has on the test results, the each share of P_{in} component test results obtained after the A40%, A60% and A80% compaction process were averaged (Gavg). The results of the P_{abs} after averaging are shown in Figure 10, Figure 11 shows P_{ref} and Figure 12 shows P_{out}.

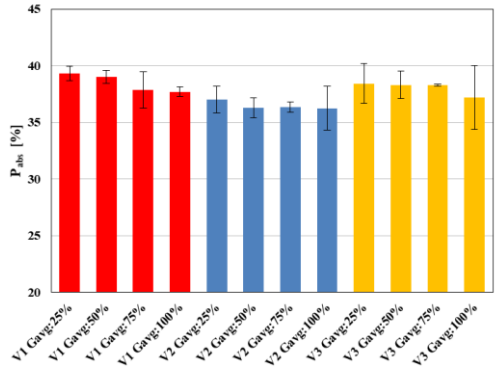

Fig. 10. The results of the study of the influence of PLA wall positioning variants and infill densities (25%, 50%, 75%, 100%) on the absorption of microwaves expressed by P_{abs} value after averaging the apparent density

From the Gavg analyses (Fig. 10) for the averaged P_{abs}, it can be seen that the PLA-wall position variants used in V1, V2 and V3, as well as the applied 'grid' infill inside the wall, affect the share of absorbed MW power. The position of the PLA wall in the measurement chamber closest to the microwave source (V1) most clearly shows the influence of the grid-type filling used. Grid type infill Gavg:25% is the most favourable (the highest share of P_{abs})

in all three variants, even when using two PLA walls in the V2 tests. It can also be observed that increasing the grid type filling density has the effect of reducing the microwave heating efficiency of the SSBS. The use of internal grid infill density 'Gavg:100%' is the least favourable. It can also be seen from the graph in Figure 10 that the implementation of PLA walls before and after the unhardened moulding sand in the V2 variant of the multimaterial system reduced the share of absorbed MW power. The least noticeable differences in microwave absorption are observed when using different infill grid filling of the PLA wall, which was placed at the end of the measurement chamber (after the SSBS). The effect of using different infill grid filling in the PLA walls is also visible in the share of P_{ref} reflected power in the V1, V2 and V3 variants (see Fig. 11). Grid type infill density Gavg:25% is the most favourable (the lowest share of P_{ref}) in all three tested V-variants. Placing the PLA wall at the end of the waveguide (V3 - after the SSBS), reduced the share of P_{ref} (Fig. 12) even below 35%. In this V3 variant, the impact of the use of different infill density was the lowest among the other tested variants: V1 and V2.

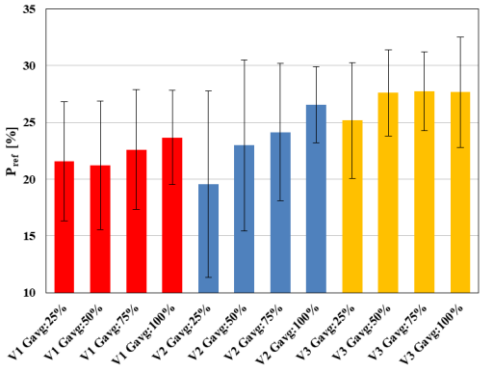

Fig. 11. The results of the study of the influence of PLA wall positioning variants and infill densities (25%, 50%, 75%, 100%) on the reflection of microwaves expressed by P_{ref} value after averaging the apparent density

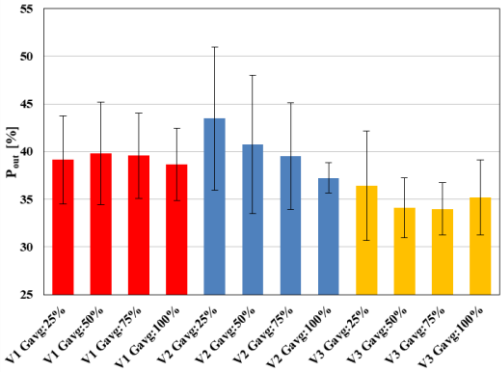

Fig. 12. The results of the study of the influence of PLA wall positioning variants and infill densities (25%, 50%, 75%, 100%) on the output power of microwaves expressed by P_{out} value after averaging the apparent density

Figure 13 shows the condition of the PLA wall surface after the executed test plan. The wall surface was not cleaned mechanically. Any loose objects on the PLA wall surface were cleaned with a jet of compressed air and then subjected to SEM examination.

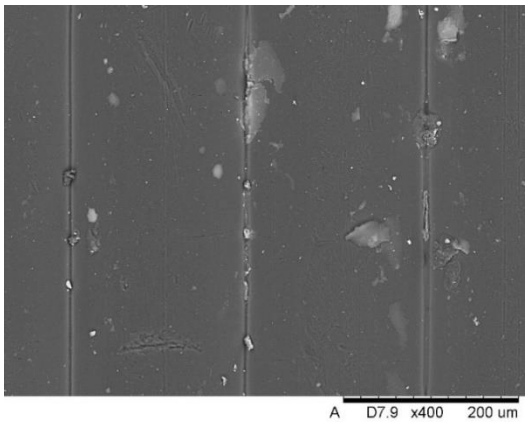

Fig. 13. SEM observations of the PLA wall surface after tests with some contaminants accumulating in the spaces between the layers of applied material in FDM technique

SEM observations revealed the presence of contamination within the welds between the individual layers of applied PLA (Fig. 13). Figure 14 shows the state of PLA wall surface after 3D reconstruction method.

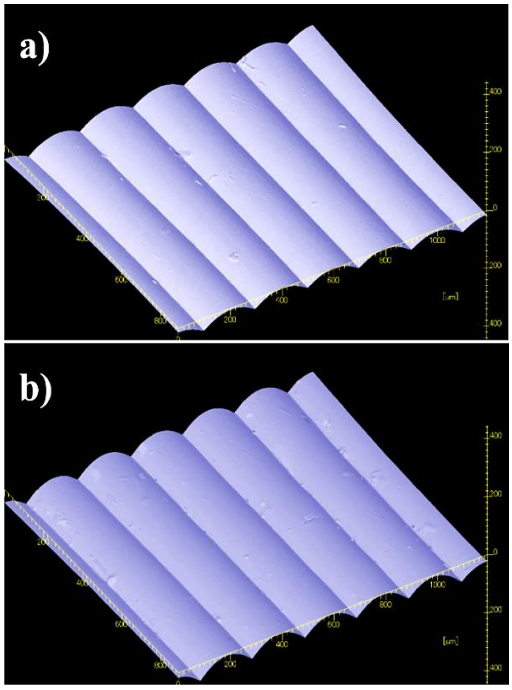

Fig. 14. View of the examples of PLA FDM printed walls: a) infill 25%, b) infill 100% with no surface abrasive defects. 3D reconstruction shows that layer high at 0.2 mm are repetitive

State of 3D-reconstructed surface of PLA walls (Fig. 14) shows that, during moulding and compacting SSBS there were no significant abrasive wear places.

4. Conclusions

The presented results of the research on effectiveness of absorbing microwaves by the multimaterial sodium silicate base sand - PLA mould wall systems lead to the following conclusions:

- Measurement results for RL and IL loss factors of microwave radiation in microwave slot line chamber make it possible to forecast, on the grounds of calculated absorbed power share (P_{abs}), effectiveness of heating with microwaves 2.45 GHz at the level between 36% and 40% of P_{in} power for density of unhardened moulding sands between 1.19 and 1.53 g/cm^3 closed with 5mm PLA wall/walls. Obtained P_{abs} results, in general, are only slightly worse than the tests carried out on SSBS [4] without PLA walls.
- Calculated Gavg analyses for the averaged P_{abs} proves that the PLA-wall position variants used in V1, V2 and V3, as well as the applied 'grid' infill density inside the wall have a limited effect on the share of absorbed MW power (P_{abs}). In conjunction with the low tangent loss factor there are no objections to using PLA for tools (moulds, core boxes) working in MW field, as long as their maximum work temperatures are respected.
- Use of the two PLA-walls in V2 variant of the multimaterial SSBS-PLA system most visibly (c.a. 3%) reduced the share of absorbed MW power (P_{abs}).
- Decrease in share of P_{abs} are connected with increase of infill density of the 5 mm 3DP PLA-walls. The use of internal grid infill density at 'Gavg:100%' was the least favourable in all tested V-variants.
- Use of compaction amplitude from A40% to A80% effect in increasing of apparent density of the SSBS. The share of P_{ref} in analysed variant: V1, V2 and V3 was the highest at 'Gavg:100%' in which the share of output power (P_{out}) was usually the lowest.
- All of the 'V3 Gavg' results of P_{ref} share were the highest, and so P_{out} share were the lowest.
- From the viewpoint of effectiveness of microwave heating of unhardened moulding sands in SSBS – PLA systems, decreasing P_{ref} share in favour of P_{out} can be of high practical importance for hardening medium and large-size moulds and cores in V1 and V2 variants of placing the PLA wall/walls.
- Research should be extended to other types of infill patterns, base sands, sodium silicate binders and shapes of PLA –walls to determine their effect on the components of P_{in}.

Acknowledgement

The research was financially supported from the grant for statutory activity No. 8211104160.

References

[1] Stachowicz, M., Opyd, B., Granat, K., & Markuszewska, K. (2014). Effect of electrical properties of materials on effectiveness of heating their systems in microwave field. *Archives of Foundry Engineering.* 14(2), 111-114. DOI: 10.2478/afe-2014-0047.

[2] Stachowicz M., Mażulis J., Granat K. & Janus A. (2014). Influence of molding and core sands matrix on the effectiveness of the microwaves absorption. *Metalurgija*. 53(3), 317-319. ISSN 0543-5846.

[3] Stachowicz M. & Granat K. (2013). Microwave absorption by unhardened molding sands with water-glass. *Archives of Foundry Engineering.* 13(spec.1), 169-174. (in Polish).

[4] Stachowicz, M. (2016). Effect of sand base grade and density of moulding sands with sodium silicate on effectiveness of absorbing microwaves. *Archives of Foundry Engineering*, 16(3), 103-108. DOI: 10.1515/afe-2016-0059.

[5] Kaczmarska, K., Grabowska, B., Spychaj, T., Zdanowicz, M., Sitarz, M., Bobrowski, A. & Cukrowicz, S. (2018). Effect of microwave treatment on structure of binders based on sodium carboxymethyl starch: FT-IR, FT-Raman and XRD investigations. *Spectrochimica Acta Part A: Molecular and Biomolecular Spectroscopy*, 199, 387-393. https://doi.org/10.1016/j.saa.2018.03.047.

[6] Puzio, S., Kamińska, J., Major-Gabryś, K., Angrecki, M. & Hosadyna-Kondracka, M. (2019). Microwave-Hardened Moulding Sands with Hydrated Sodium Silicate for Modified Ablation Casting. *Archives of Foundry Engineering*. (2), 91-96. DOI: 10.24425/afe.2019.127122.

[7] Solonenko, L., Repiakh, S., Uzlov, K. & Kimstach, T. (2020). Crushing character of sand-sodium-silicate mixtures structured by steam-microwave treatment. *Odes'kyi Politechnichnyi Universytet. Pratsi*. 3(62), 5-14. DOI: 10.15276/opu.3.62.2020.01.

[8] Major-Gabryś, K., Hosadyna-Kondracka, M., Grabarczyk, A. & Kamińska, J. (2019). Selection of hardening technology of moulding sand with hydrated sodium silicate binder devoted to aluminum alloys ablation casting. *Archives of Metallurgy and Materials*. 64(1), 359-364. DOI: 10.24425/amm.2019.126260 ; ISSN 1733-3490.

[9] Fortini, A., Merlin, M. & Raminella, G. (2022). A comparative analysis on organic and inorganic core binders for a gravity diecasting Al alloy component. *International Journal of Metalcasting*. 16(2), 674-688. DOI: https://doi.org/10.1007/s40962-021-00628-1.

[10] Banganayi, F.C., Nyembwe, D.K. & Polzin, H. (2020). Optimisation of an environmentally friendly foundry inorganic binder core making process for the replacement of an organic binder. *MRS Advances*. 5(25), 1323-1330. DOI: https://doi.org/10.1557/adv.2020.225.

[11] Grabowska, B., Kaczmarska, K., Cukrowicz, S., Mączka, E. & Bobrowski, A. (2020). Polylactide used as filment in 3D printing–part 1: FTIR, DRIFT and TG-DTG studies. *Journal of Casting & Materials Engineering*. 4(3), 48-52. DOI: https://doi.org/10.7494/jcme.2020.4.3.48.

[12] Ullah, S., Flint, J.A. (2014). Electro-textile based wearable patch antenna on biodegradable poly lactic acid (PLA) plastic substrate for 2.45 GHz, ISM band applications. In *2014 International Conference on Emerging Technologies (ICET)* (pp. 158-163). IEEE. DOI: 10.1109/ICET.2014.7021036.

[13] Ahmad, M.S., Abdelazeez, M.K. & Zihlif, A.M. (1989). Microwave properties of the talc filled polypropylene. *Journal of Materials Science*. 24, 1795-1800.
[14] Szczepanik, S., & Nikiel, P. (2020). Influence of structural characteristics on the mechanical properties of FDM printed PLA material. *Journal of Casting & Materials Engineering*, 4(1), 1-8. DOI: https://doi.org/10.7494/jcme.2020.4.1.1.
[15] Tanveer, M.Q., Mishra, G., Mishra, S. & Sharma, R. (2022). Effect of infill pattern and infill density on mechanical behaviour of FDM 3D printed Parts-a current review. *Materials Today: Proceedings*. 62(1), 100-108. DOI: https://doi.org/10.1016/j.matpr.2022.02.310.
[16] Wang, S., Ma, Y., Deng, Z., Zhang, S., & Cai, J. (2020). Effects of fused deposition modeling process parameters on tensile, dynamic mechanical properties of 3D printed polylactic acid materials. *Polymer testing*, 86, 106483. DOI: https://doi.org/10.1016/j.polymertesting.2020.106483.